Journal of the European Ceramic Society 45 (2025) 117189

Contents lists available at ScienceDirect

Journal of the European Ceramic Society

journal homepage: www.elsevier.com/locate/jeurceramsoc

Axial plasma spraying of aqueous solution precursors: A facile approach for columnar thermal barrier coatings

Thomas Hervy [a,b], Nicholas Curry [c], Stefan Björklund [a], Frantisek Lukac [d], Shrikant Joshi [a,*]

[a] Department of Engineering Science, University West, Sweden
[b] Department of Mechanical Engineering, University of Limoges, France
[c] Thermal Spray Innovations, Salzburg, Austria
[d] Institute of Plasma Physics of the Czech Academy of Sciences, Prague, Czech Republic

ARTICLE INFO

Keywords:
Thermal barrier coating
Solution precursor plasma spraying
Axial injection
Columnar microstructure
XRD
Deposition rate
Thermal cycling
YSZ

ABSTRACT

Thermal barrier coatings (TBC) are an essential part of modern gas turbines for aviation and power generation. As such, there is an incessant demand for improved TBC performance and longevity. Of the possible coating microstructures, the columnar structure first produced by electron beam physical vapour deposition was found to be most durable. The subsequently developed suspension plasma spray coatings are seen as an alternative method for producing columnar TBCs but typically utilise flammable solvents to achieve such structures. Aqueous solution precursors have also been used as a feedstock to deposit yttria stabilised zirconia (YSZ) TBCs; however, columnar structures have proven elusive, with solution precursor plasma spray (SPPS) deposition conditions and throughputs involving radial feed spray torches also being industrially unattractive. This study illustrates the first columnar coatings of single-layer yttria stabilised zirconia from an aqueous solution precursor using an axial feed capable plasma torch. Coatings have been shown to be columnar structured over a robust operating window, fully tetragonal in phase constitution and capable of being deposited at rates that can be commercially interesting. These initial results lay a great foundation for further TBC development utilizing an aqueous, powder-free, feedstock.

1. Introduction

Since the 1980s, Thermal Barrier Coatings (TBCs) have been applied to nickel-based superalloy parts in gas turbines to prevent premature degradation at high temperatures by providing an insulating layer, thus extending component life [1]. TBCs typically consist of a metallic bond coat and a ceramic top-coat. The bond coat, often an MCrAlY (M = Co and/or Ni), reduces thermal strain between the substrate and top coat while also providing oxidation resistance [2]. The ceramic top coat, usually yttria-stabilized zirconia (YSZ), offers low thermal conductivity, high thermal expansion, a high melting point, and good mechanical properties like erosion resistance [3].

Atmospheric Plasma Spraying (APS) and Electron Beam–Physical Vapor Deposition (EB-PVD) are the main processes for manufacturing TBCs. APS produces coatings with a lamellar structure and about 15 % porosity, which lowers thermal conductivity but can reduce thermal cyclic life and increase erosion susceptibility [4]. Dense Vertically Cracked (DVC) TBCs offer better strain tolerance but have higher thermal conductivity due to their denser structure [5]. EB-PVD TBCs have a columnar microstructure that provides higher thermal cycling life and superior erosion resistance compared to APS TBCs. However, they also have higher thermal conductivity and lower deposition rates (~3.4–10 μm/min), require high capital investment, and involve complex operations, driving the search for alternative methods [6].

Suspension Plasma Spraying (SPS) is a newer deposition method that can combine the benefits of APS and EB-PVD structures. Using a liquid carrier to transport fine ceramic particles into the plasma jet, the SPS process can produce coatings with varying microstructures, columnar structured coatings in particular [7]. Such columnar SPS coatings have shown comparable or superior properties to APS and EB-PVD coatings, such as higher porosity, lower thermal conductivity, and finer microstructures [8].

Solution Precursor Plasma Spraying (SPPS) is an alternative liquid feedstock based method, using a precursor salt solution instead of suspension of particles, that has been demonstrated to be capable of depositing ceramic TBC layers. The precursors have the advantage of

* Corresponding author.
E-mail address: shrikant.joshi@hv.se (S. Joshi).

https://doi.org/10.1016/j.jeurceramsoc.2025.117189
Received 21 August 2024; Received in revised form 31 December 2024; Accepted 5 January 2025
Available online 8 January 2025

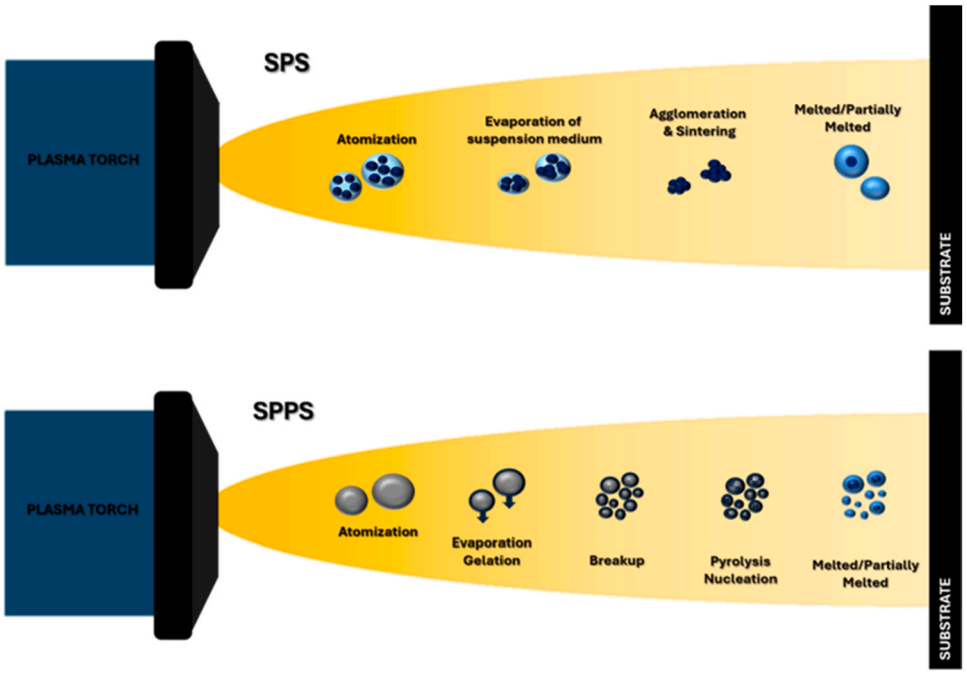

Fig. 1. Schematic illustration of coating formation during SPS and SPPS.

being aqueous, stable and avoid sedimentation issues found with suspensions, while using the same equipment as SPS. As illustrated in Fig. 1, the solution precursors must undergo additional nucleation and pyrolysis steps to form ceramic particles, a process influenced and hampered by the limited residence time in the plasma jet. While SPS has successfully produced columnar coatings from a variety of feedstocks [7,8], including in some cases with water-based suspensions [9,10], SPPS has not yet demonstrated this capability especially with single-layer YSZ, the workhorse composition of the turbine industry [11,12].

It is pertinent to mention that SPPS has demonstrated the capability to create other interesting microstructures for TBCs. Kumar et al. have demonstrated Yttrium Aluminium Garnet coatings with SPPS, which exhibit a mixed structure with highly prominent Inter-Pass Boundaries (IPB) [13]. This approach with SPPS has been further validated for use as a TBC on various engine components [14]. In other works, solution precursors have been used to add layers to an already deposited SPS coating [15]. In very rare cases, columnar coatings have also been reported but this has been in coating compositions other than YSZ, such as lanthanum zirconate and barium magnesium tantalate [16,17].

A vast majority of previous SPPS research has utilised radial injection of solution precursors [11,12]. However, radial injection has inherent challenges in introducing the solution into the hot core of the plasma jet, relying entirely on the plasma plume for atomisation and limiting the control of droplet size. This also prevents complete utilization of thermal energy available in the plasma plume that is critical when additional steps such as nucleation and pyrolysis are to be accomplished during the short residence time. Axial injection plasma guns, by contrast, can inject the solution directly into the plasma core, provide optimal ability to produce fine droplets and better facilitate the gas-droplet/solid transport processes in flight. Prior studies have already demonstrated in flight formation of sub-micron YSZ particles during SPPS [14]. Based on the now well-accepted mechanism responsible for column formation in SPS [7], drag forces of the impinging plasma can cause such fine particles to deviate from the spray direction to preferentially impact on substrate asperities and facilitate deposits that ultimately lead to columnar growth. Therefore, if the processing conditions are suitable to induce in flight fine particle formation from solution precursors as mentioned above [14], it is reasonable to imagine that SPPS with YSZ precursors

Table 1
Parameters used for deposition of TBCs and measured coating properties.

Nomenclature	Spraying Parameters							Coating Properties			
	Nozzle Diameter (Inch)	Total Gas Flow (l/min)	Net Power (kW)	Solution feed (ml/min)	Equivalent Solids (g/min)	Stand-Off Distances (mm)	Coating Passes	Thickness (μm)	Thickness per Pass (um)	Total Porosity (%)	Estimated Deposition Efficiency
Run 1	3/8	300	65	80	21.1	90	60	138.6	2.31	17.6	53 %
						80		162.0	2.70	17.9	65 %
						70		172.2	2.87	22.5	72 %
						60		180.0	3.00	18.3	89 %
Run 2	3/8	280	67	80	21.1	100	80	137.6	1.72	17.2	40 %
						90		160.8	2.01	13.6	53 %
						80		184.8	2.31	13.4	66 %
						70		204.0	2.55	15.6	76 %
Run 3	5/16	250	54.2	75	19.8	70	40	76.8	1.92	25.0	51 %
						60		93.2	2.33	21.9	61 %
						50		106.0	2.65	27.1	76 %
						40		118.8	2.97	31.1	83 %

too should be able to realize columnar microstructures similar to those reported via SPS. The above hypothesis has motivated the present study which represents an initial attempt at producing columnar YSZ coatings with a solution precursor, utilising an axial injection plasma system. Of particular note is the use of an aqueous solution precursor that removes the safety concerns associated with using a flammable suspension.

2. Experimental

2.1. Preparation of SPPS coatings

Hastelloy-X and Domex 355 MC substrates of 25.4 mm diameter and 6 mm thickness were grit blasted using alumina grit to a surface roughness (Ra) of approximately 3 μm before bond coat deposition. The commercially available NiCoCrAlY powder (AMDRY 386, Oerlikon Metco, Switzerland) was used as a metallic bond coat and sprayed on the substrates using a high-velocity air fuel (HVAF) spray torch (M3 system, UniqueCoat, USA).

Solution precursor yttria stabilised zirconia feedstock was prepared by mixing Yttrium Acetate ($C_6H_9O_6Y$) and Zirconium Acetate ($C_8H_{12}O_8Zr$), both from Treibacher Industrie AG (Austria), proportionally to theoretically yield 8 wt% yttrium oxide content in the zirconia matrix. This prepared solution had an equivalent solids load of 14,9 wt% YSZ, assuming complete stoichiometric conversion to the corresponding oxides.

An Axial III Plus high-power plasma torch (Northwest Mettech Corp., Canada) equipped with a Nanofeed 350 feeding system was used to process the solution precursor. Three sets of process parameters, designated as Run 1, Run 2 and Run 3, were used to produce coatings as shown in Table 1. Samples were coated on a rotating turntable using a specially designed fixture that allowed for coatings to be deposited at 4 different spray distances simultaneously.

2.2. Sample preparation and microstructural analysis

Coated samples were prepared for cross-section examination following a standard double mounting procedure used for TBCs, involving vacuum mounting in epoxy, sectioning and remounting before grinding and polishing. SEM analysis was performed using a TM3000 (Hitachi High-Tech Europe GmbH, Germany) coupled with energy-dispersive spectroscopy (EDS) unit (Quantax XFFlash MIN SVE, Bruker, Germany) after gold sputtering. For each coating, a minimum of 10 micrographs were taken to provide a statistically reliable porosity evaluation. These micrographs were further evaluated using the ImageJ software (National Institutes of Health, USA) and an automated image processing routine used to auto threshold microstructure images into binary to identify pores and cracks, for measuring their ratio. The column or segmentation density was measured according to the method reported previously by Algenaid et al. [18]. A straight line of known length was drawn through the middle of the ceramic top-coat layer thickness. All the column boundaries that intersected the mentioned line were counted. The resulting column density was then calculated using Eq. (1).

$$column\ density = \frac{(No.of\ column\ boundaries\ intersecting\ the\ line - 1}{True\ lenght\ of\ the\ line} \quad (1)$$

2.3. XRD analysis

Phase compositions of coated samples were determined by powder X-ray diffraction (PXRD) methods. The measurements were carried out on a vertical powder θ-θ diffractometer D8 Discover (Bruker AXS, Germany) using Cu Kα radiation with Ni Kβ filter in the range from 15° to 110°. The phase identification was performed using the X'Pert HighScore software (Malvern Panalytical, Ltd., U.K.). Chemical composition of coatings was determined using an X-ray fluorescence (XRF) analyser Bruker S2 Puma (Bruker AXS, DE).

Table 2
Comparison of deposition efficiency and deposition rate achieved in the present study with values reported in prior SPS studies.

	Solids Load	Feed Rate of Ceramic (g/min)	Deposition Efficiency	Deposition Rate (g/min)
This study	14.9 %	21.1	65 %	13.72
Curry et al. [20]	25 %	26.0	54.2 %	14.09
Chen & Dambra [21]	25 %	7.5	51 %	3.83

3. Results and discussion

3.1. Microstructure analysis

Table 1 summarises the basic measurements for the 12 coatings (3 gun parameters, 4 spray distances for each parameter) produced in this study, including the coating thickness, deposition rate, total porosity and estimated deposition efficiency. It is to be noted that samples were sprayed in rotation using a fixture that can simultaneously accommodate samples at 4 different spray distances. As the fixture rotates at a fixed RPM, each of the 4 different standoff distances results in different surface speeds, with the shortest standoff distance corresponding to the highest surface speed.

It can be observed that, in each run, the deposition rate increases with shorter standoff distance. This is despite the fact the samples deposited with a shorter stand-off distance correspond to a higher surface speed as described above, a factor that should typically result in a lower thickness per pass. This further highlights the influence of stand-off distance. Deposition efficiency, estimated according to the method presented by Trache et al. [19], is also observed to increase with reduced stand-off distance. It is pertinent to note that a typical state-of-art columnar SPS TBC produced with the same axial injection equipment has a deposition efficiency of 54.2 % [20]. Other researchers have reported a similar level of efficiency with radial injection of suspensions, though at a much lower feed rate (nearly by a factor of 3) [21]. For SPPS coatings, deposition efficiencies have been reported only in some cases; these are in the region of 26 %-46 % with radial injection, although these studies report non-columnar coatings [13,22]. Table 2 displays a comparison of the deposition efficiency and final deposition rate for the coatings in this work, as well as previously referenced research with SPS [20,21]. For the previously published SPS work, the feed rate and solids load data provided in each reference has been used to calculate the ceramic feed rate and this is then combined with the reported deposition efficiency to determine the deposition rate. What is clear is that, even at this early stage of development, the deposition rates for the columnar SPPS coatings are at a level equivalent to the state-of-art axial injection SPS coatings, thus indicating their industrial relevance.

Fig. 2 displays an overview of the microstructures for all 12 coatings produced in this study. In general, all of the coatings exhibit a columnar-like structure, with some variations between each run and stand-off distance, very similar to columnar coatings reported using suspensions. To date, there have been no reports of such microstructures produced with solution precursors for single-layer yttria stabilised zirconia coatings. For Run 1, a typical columnar coating is seen at 90 mm and 80 mm standoff, with the microstructure transitioning from a columnar coating to a cracked-columnar coating at 70 mm and 60 mm standoff. For Run 2, the coatings are columnar across the studied deposition window (100 mm to 70 mm standoff distance), with the columns only becoming more tightly packed as standoff distance is reduced. These SPPS coatings are comparable to those reported for columnar coatings

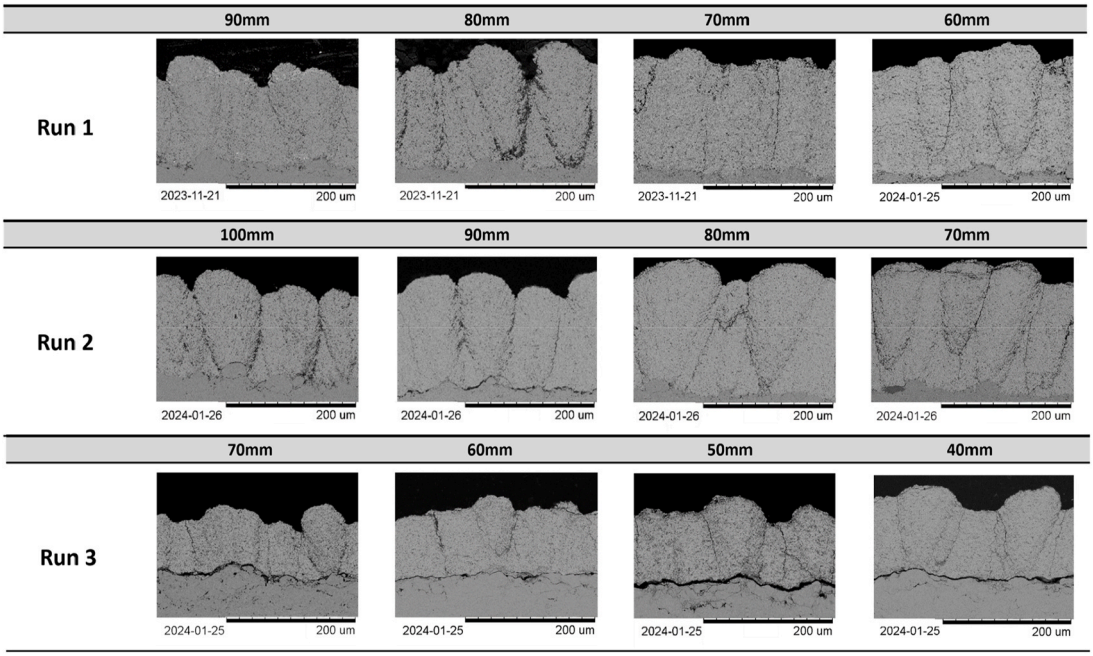

Fig. 2. SEM cross-sections revealing columnar structures in SPPS-YSZ coatings.

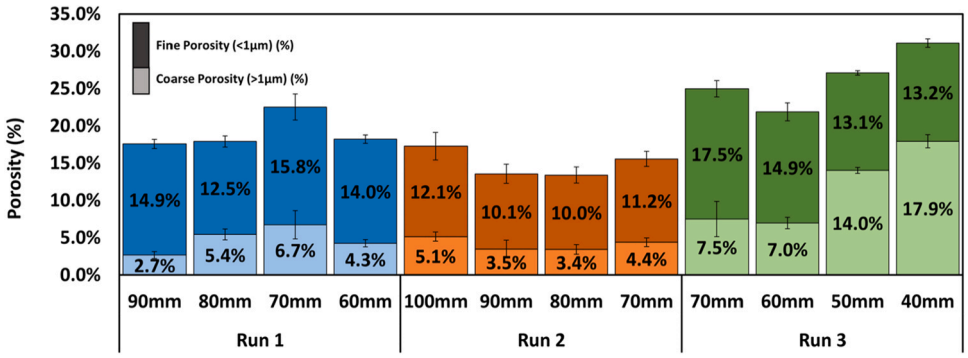

Fig. 3. Measured fine and coarse porosity in as-sprayed SPPS-YSZ TBCs.

manufactured with suspensions previously [20,23,24].

For Run 3, the coatings display a cracked-columnar structure across the investigated stand-off window (40–70 mm). This is a transitional structure between columnar and vertically cracked morphologies. A similar microstructure has been observed in SPS studies such as those reported by Curry et al. [25]. In this case, the difference in microstructure may be due to the use of a smaller plasma exit nozzle for Run 3. A smaller plasma exit nozzle will increase the plasma velocity at the solution injection point, potentially improving the atomisation process. However, the higher velocity will also reduce the time of flight for the particles and increase their velocity at the deposition standoff distance, relative to Runs 1 and 2. This higher velocity deposition is likely to result in more direct impact of the particles and reduction in columnar features due to the lower impact of the boundary layer [7].

In a number of instances there is evidence of a separation between the bond coat and the SPPS layer in the microstructure images. The gap

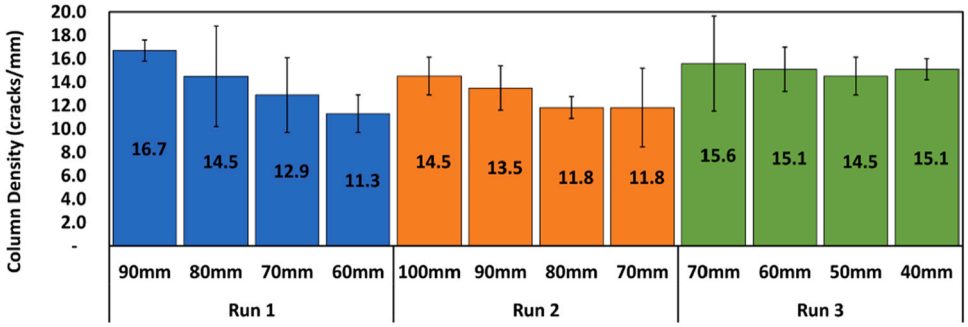

Fig. 4. Column density in as-sprayed SPPS-YSZ TBCs.

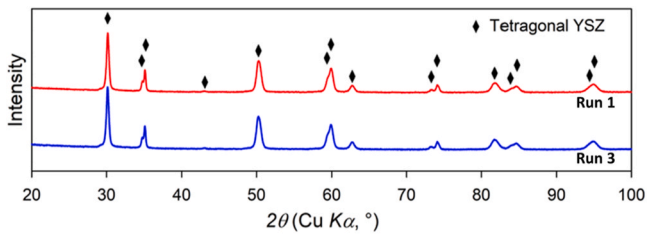

Fig. 5. XRD diffractograms of the as-sprayed SPPS-YSZ TBCs.

between layers does not contain mounting epoxy, although the coating was fully infiltrated during microstructure preparation. This suggests that the delamination occurred during the resin curing or during the subsequent cutting step and is not a part of the initial coating structure.

3.2. Porosity evaluation

Porosity has been measured at two distinct length scales and is presented in Fig. 3. This classification was done to differentiate the micrometric and sub-micron sized pores. Based on the fact that columns gaps and cracks are the primary contributors to the coarse (micrometric) porosity, it was important to separate this coarse porosity from the finer porosity that forms the column structure [26]. For Run 1 and Run 2 samples, the porosity appears to be at a similar level regardless of the standoff distance for the evaluated sample. Overall, the fine porosity (<1 μm) contributes a larger portion of the total porosity compared to the coarse (>1 μm) porosity. The values remain broadly within the range reported by previous studies for SPS, with values ranging from 11 % to 35 %. For the cracked-columnar coatings (Run 3), a different trend emerged with a decreasing fine porosity and increasing coarse porosity as the standoff distance decreased.

3.3. Column density

In TBCs with columnar microstructures, the column density is found to be an important factor governing the lifetime in thermal cycling tests, by improving the strain-tolerance of the coating structure [27]. Column density for the investigated SPPS coatings is displayed in Fig. 4. For Run 1 and Run 2, the trend revealed reducing column density with shorter standoff distance. The Run 3 deposition conditions however resulted in a relatively consistent segmentation density (from 14.5 to 15.6 cracks/mm). Previous analysis of SPS coatings has given a range of column densities, with Curry et al. [24] stating a column density of 9–12 columns/mm, and Zhou et al. [28] presenting a density of 7.5–12 columns/mm. Thus, the SPPS-based columnar YSZ TBC's reported herein can be said to have a comparable or greater column density than their SPS counterparts.

3.4. Phase constitution

Phase analyses was carried out using X-ray diffraction on both Run 1 and Run 3 samples. The analysis shown in Fig. 5 revealed that all the coatings are composed of tetragonal (t') YSZ phase desired to provide their performance in cycling thermal exposure [29]. Moreover, XRF chemical analysis of the coatings gave an average yttrium oxide content of 7.8 % ± 0.17 %, 2.02 % ± 0.07 % hafnium oxide and the balance zirconia. This further confirms that the required coating chemistry (6–8 wt% YSZ) was achieved during spray processing.

4. Conclusions

This study explored the formation of columnar microstructures in Yttria-Stabilized Zirconia (YSZ) Thermal Barrier Coatings (TBCs) using aqueous Solution Precursor Plasma Spraying (SPPS) with axial injection. Experimental results demonstrate for the first time that SPPS can indeed produce columnar microstructures over a wide process window, with three parameter variations exhibiting columnar or cracked-columnar structures with a segmentation density comparable to or higher than that reported by SPS. Further analysis confirmed the presence of the tetragonal YSZ phase, crucial for TBC performance.

This study establishes that SPPS with axial injection is a viable method for producing columnar YSZ TBCs using an aqueous solution precursor, contrasting with the conventional flammable ethanol solvent typically used for SPS. These findings provide a foundation for further evaluation for axial injection SPPS. Future work will focus on refining the process window and comparing their performance with benchmark SPS coatings.

CRediT authorship contribution statement

Shrikant Joshi: Writing – review & editing, Supervision, Resources, Project administration, Methodology, Conceptualization. **Frantisek Lukac:** Visualization, Methodology, Formal analysis. **Stefan Björklund:** Methodology, Investigation, Data curation. **Nicholas Curry:** Writing – review & editing, Visualization, Formal analysis. **Thomas Hervy:** Writing – original draft, Visualization, Investigation, Formal analysis, Data curation.

Declaration of Competing Interest

The authors declare that they have no known competing financial interests or personal relationships that could have appeared to influence the work reported in this paper.

Acknowledgments

The authors would like to acknowledge the financial support from the Knowledge Foundation (grant number 20220171). The authors would like to thank their colleagues at University West, Dr Tunji Owoseni, Dr Madhura Bellippady and Magnus Sandberg, for their assistance with precursor preparation, characterization and spraying of coatings, respectively. The help rendered by Dr Radek Musalek and Dr Romain Genois for the characterization at the Institute of Plasma Physics is also gratefully acknowledged.

References

[1] A. Bennett, F.C. Roriz, A.B. Thakker, A philosophy for thermal barrier coating design and its corroboration by 10 000h service experience on RB211 nozzle guide vanes, Surf. Coat. Technol. 32 (1987) 359–375, https://doi.org/10.1016/0257-8972(87)90120-4.
[2] J.G. Thakare, C. Pandey, M.M. Mahapatra, R.S. Mulik, Thermal barrier coatings—a state of the art review, Met. Mater. Int. 27 (2021) 1947–1968, https://doi.org/10.1007/s12540-020-00705-w.
[3] E. Bakan, R. Vaßen, Ceramic top coats of plasma-sprayed thermal barrier coatings: materials, processes, and properties, J. Therm. Spray. Tech. 26 (2017) 992–1010, https://doi.org/10.1007/s11666-017-0597-7.
[4] S. Mahade, A. Venkat, N. Curry, M. Leitner, S. Joshi, Erosion performance of atmospheric plasma sprayed thermal barrier coatings with diverse porosity levels, Coatings 11 (2021) 1–21.
[5] H.B. Guo, R. Vaßen, D. Stöver, Atmospheric plasma sprayed thick thermal barrier coatings with high segmentation crack density, Surf. Coat. Technol. 186 (2004) 353–363, https://doi.org/10.1016/j.surfcoat.2004.01.002.
[6] A. Feuerstein, J. Knapp, T. Taylor, A. Ashary, A. Bolcavage, N. Hitchman, Technical and economical aspects of current thermal barrier coating systems for gas turbine engines by thermal spray and EBPVD: a review, J. Therm. Spray. Tech. 17 (2008) 199–213, https://doi.org/10.1007/s11666-007-9148-y.
[7] K. VanEvery, M.J.M. Krane, R.W. Trice, H. Wang, W. Porter, M. Besser, D. Sordelet, J. Ilavsky, J. Almer, Column formation in suspension plasma-sprayed coatings and resultant thermal properties, J. Therm. Spray. Tech. 20 (2011) 817–828, https://doi.org/10.1007/s11666-011-9632-2.
[8] R.S. Lima, B.M.H. Guerreiro, M. Aghasibeig, Microstructural characterization and room-temperature erosion behavior of as-deposited SPS, EB-PVD and APS YSZ-based TBCs, J. Therm. Spray. Tech. 28 (2019) 223–232, https://doi.org/10.1007/s11666-018-0763-6.
[9] A. Yaghtin, M. Yaghtin, P. Najafisayar, Z. Tang, T. Troczynski, On the applicability of modified water-based yttria-stabilized zirconia suspensions to produce plasma-

sprayed columnar coatings, Coatings 13 (2023) 1330, https://doi.org/10.3390/coatings13081330.
[10] P. Xu, G. Meng, G. Liu, T. Coyle, L. Pershin, J. Mostaghimi, Columnar-structured thermal barrier coatings deposited via the water-based suspension plasma spray process, J. Phys. D: Appl. Phys. 55 (2022) 204001, https://doi.org/10.1088/1361-6463/ac4721.
[11] E.H. Jordan, C. Jiang, M. Gell, The solution precursor plasma spray (SPPS) process: a review with energy considerations, J. Therm. Spray. Tech. 24 (2015) 1153–1165, https://doi.org/10.1007/s11666-015-0272-9.
[12] S. Govindarajan, R.O. Dusane, S.V. Joshi, In situ particle generation and splat formation during solution precursor plasma spraying of yttria-stabilized zirconia coatings, J. Am. Ceram. Soc. 94 (2011) 4191–4199, https://doi.org/10.1111/j.1551-2916.2011.04773.x.
[13] R. Kumar, C. Jiang, B. Cottom, M. Gell, E. Jordan, M. Ullaha, Development of Solution Precursor Plasma Spray (SPPS) Yttrium Aluminum Garnet (YAG) Coatings for Engine Components Using a High Enthalpy Cascaded Arc Gun: Part I, (2023). https://doi.org/10.1007/s11666-023-01573-7.
[14] B. Cottom, R. Kumar, C. Jiang, M. Gell, E. Jordan, Component Demonstration and Engine Validation of Solution Precursor Plasma Spray (SPPS) Yttrium Aluminum Garnet (YAG) Thermal Barrier Coatings: Part II, (2023). https://doi.org/10.1007/s11666-023-01572-8.
[15] K. Leng, A. Rincon Romero, F. Venturi, I. Ahmed, T. Hussain, Solution precursor thermal spraying of gadolinium zirconate for thermal barrier coating, J. Eur. Ceram. Soc. (2021), https://doi.org/10.1016/j.jeurceramsoc.2021.11.050.
[16] M. Yaghtin, A. Yaghtin, P. Najafisayar, Z. Tang, T. Troczynski, Deposition of columnar-morphology lanthanum zirconate thermal barrier coatings by solution precursor plasma spraying, J. Therm. Spray. Tech. (2021), https://doi.org/10.1007/s11666-021-01258-z.
[17] H. Hou, J. Veilleux, F. Gitzhofer, Q. Wang, Vertical grain and columnar structured Ba(Mg1/3Ta2/3)O3 thermal barrier coating deposited by solution precursor plasma spray, Surf. Coat. Technol. 393 (2020) 125803, https://doi.org/10.1016/j.surfcoat.2020.125803.
[18] W. Algenaid, A. Ganvir, R.F. Calinas, J. Varghese, K.V. Rajulapati, S. Joshi, Influence of microstructure on the erosion behaviour of suspension plasma sprayed thermal barrier coatings, Surf. Coat. Technol. 375 (2019) 86–99, https://doi.org/10.1016/j.surfcoat.2019.06.075.
[19] R. Trache, N. Curry, K. Körner, M. Leltner, Volume-based deposition factor- a practical approach to estimate deposition efficiency, Proc. Int. Therm. Spray. Conf. 2019-May (2019) 678–681.
[20] N. Curry, S. Mahade, A. Venkat, S. Joshi, Erosion performance of suspension plasma spray thermal barrier coatings — a comparison with state of art coatings, Surf. Coat. Technol. 437 (2022) 128311, https://doi.org/10.1016/j.surfcoat.2022.128311.
[21] D. Chen, C. Dambra, Thick columnar-structured thermal barrier coatings using the suspension plasma spray process, Coatings 14 (2024) 996, https://doi.org/10.3390/coatings14080996.
[22] R. Kumar, J. Wang, C. Jiang, D. Cietek, J. Favata, S. Shahbazmohamadi, J. Roth, M. Gell, E. Jordan, Low thermal conductivity yttrium aluminum garnet thermal barrier coatings made by the solution precursor plasma spray: part i—processing and properties, J. Therm. Spray. Technol. 27 (2018), https://doi.org/10.1007/s11666-018-0728-9.
[23] N. Curry, Z. Tang, N. Markocsan, P. Nylén, Influence of bond coat surface roughness on the structure of axial suspension plasma spray thermal barrier coatings - thermal and lifetime performance, Surf. Coat. Technol. 268 (2015) 15–23.
[24] A. Ganvir, R.F. Calinas, N. Markocsan, N. Curry, S. Joshi, Experimental visualization of microstructure evolution during suspension plasma spraying of thermal barrier coatings, J. Eur. Ceram. Soc. 39 (2019) 470–481.
[25] N. Curry, K. VanEvery, T. Snyder, N. Markocsan, Thermal conductivity analysis and lifetime testing of suspension plasma-sprayed thermal barrier coatings, Coatings 4 (2014) 630–650, https://doi.org/10.3390/coatings4030630.
[26] S. Mahade, C. Ruelle, N. Curry, J. Holmberg, S. Björklund, N. Markocsan, P. Nylén, Understanding the effect of material composition and microstructural design on the erosion behavior of plasma sprayed thermal barrier coatings, Appl. Surf. Sci. 488 (2019) 170–184, https://doi.org/10.1016/j.apsusc.2019.05.245.
[27] N. Kumar, M. Gupta, D.E. Mack, G. Mauer, R. Vaßen, Columnar thermal barrier coatings produced by different thermal spray processes, J. Therm. Spray. Tech. (2021), https://doi.org/10.1007/s11666-021-01228-5.
[28] D. Zhou, O. Guillon, R. Vaßen, Development of YSZ thermal barrier coatings using axial suspension plasma spraying, Coatings 7 (2017) 120, https://doi.org/10.3390/coatings7080120.
[29] S.A. Tsipas, Effect of dopants on the phase stability of zirconia-based plasma sprayed thermal barrier coatings, J. Eur. Ceram. Soc. 30 (2010) 61–72, https://doi.org/10.1016/j.jeurceramsoc.2009.08.008.